

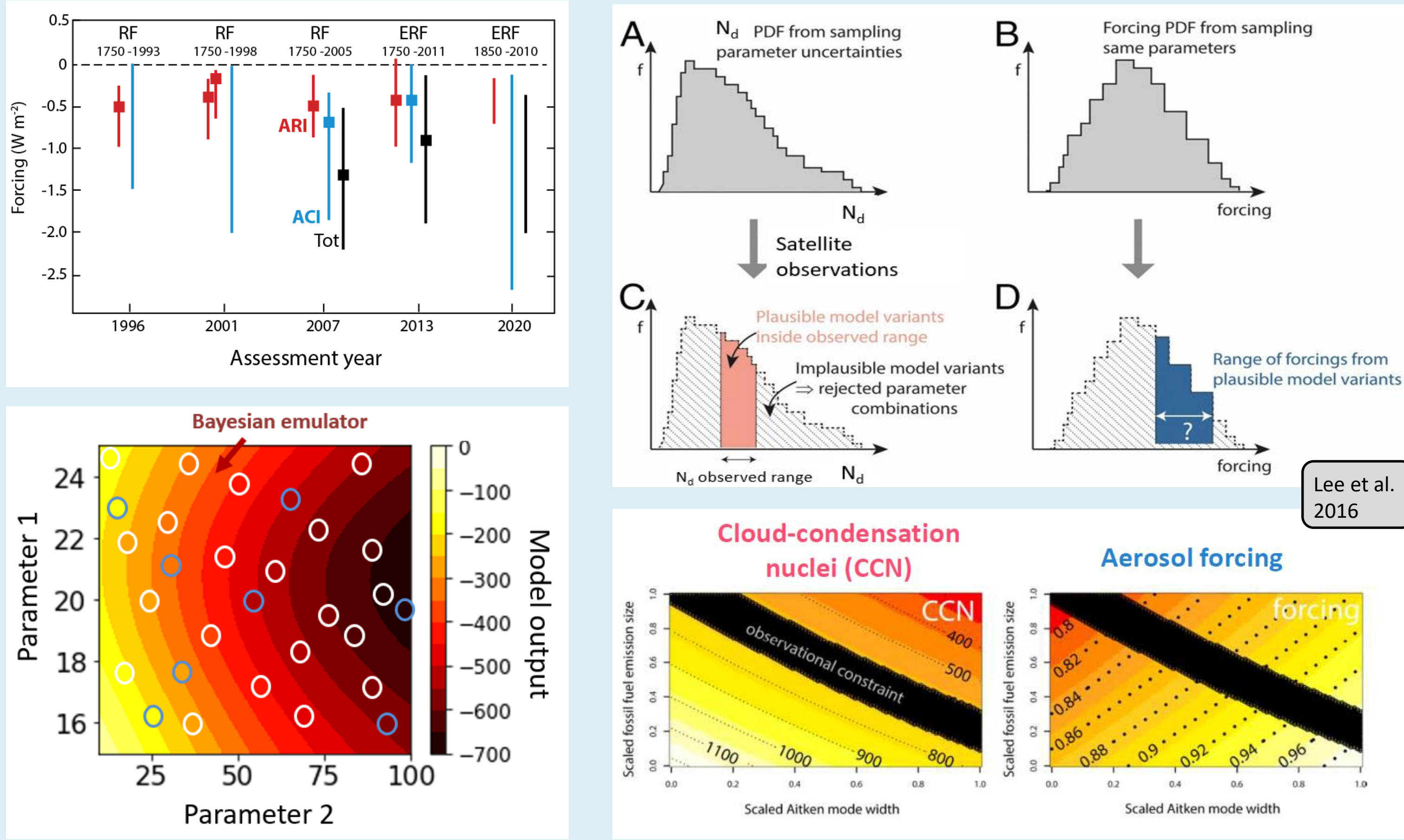
# Disentangling model structural and parametric causes of uncertainty



Leighton Regayre<sup>1,2</sup>, Kunal Ghosh<sup>2</sup>, Léa Prevost<sup>2</sup>, Jill S. Johnson<sup>3</sup>, Jeremy Oakley<sup>3</sup> and Ken Carslaw<sup>2</sup>

1: UK Met Office Hadley Centre, 2: University of Leeds, Institute for Climate and Atmospheric Science (ICAS), UK 3: University of Sheffield, School of Mathematics and Statistics, UK

## 1. Our approach to constraining aerosol-cloud interaction forcing ( $\Delta F_{aci}$ )



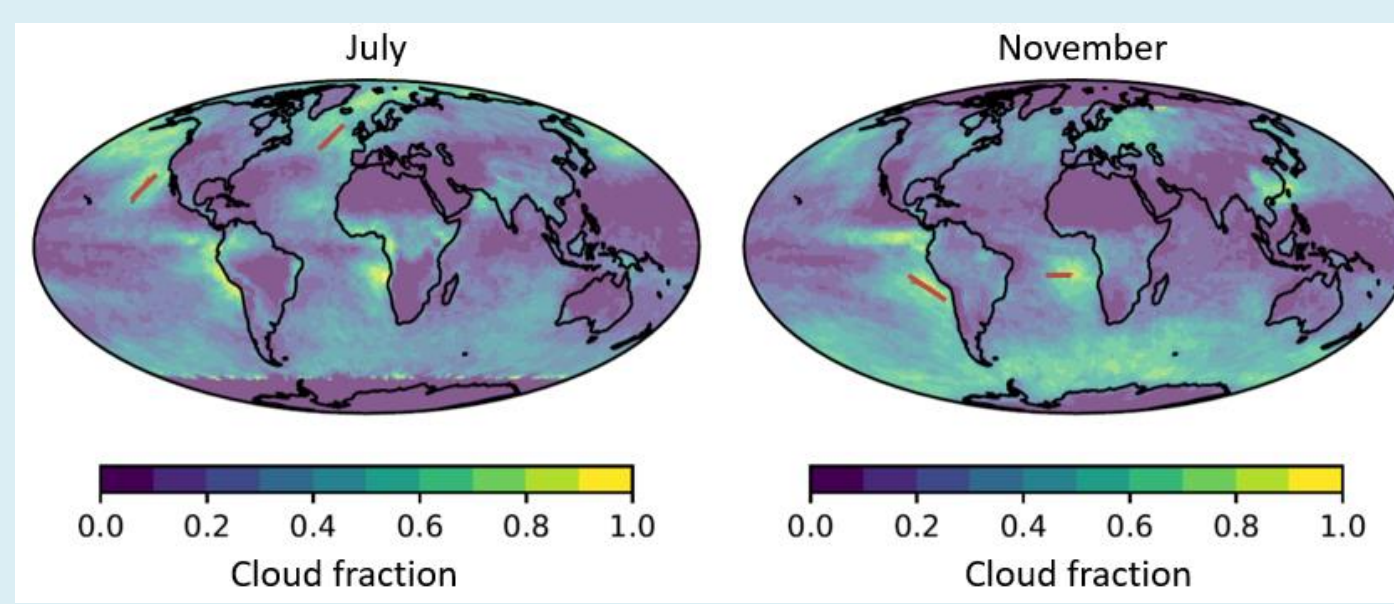
Lee et al. 2016

A perturbed parameter ensemble (221 members) and Bayesian emulation (1 million model variants) allow us to 1) quantify model parametric uncertainty, 2) challenge model variants with satellite data, 3) identify structural model inadequacies, and 4) characterize process-based limits to  $\Delta F_{aci}$  constraint

## 2. Satellite-derived observational constraints

More than 450 satellite-based observations in 5 regions used to challenge 1M model variants:

- Transects from St. to Cu. regions
- Monthly and annual mean, and seasonal amplitude of state variables
- Hemispheric difference in cloud drop concentrations ( $H_d$ )

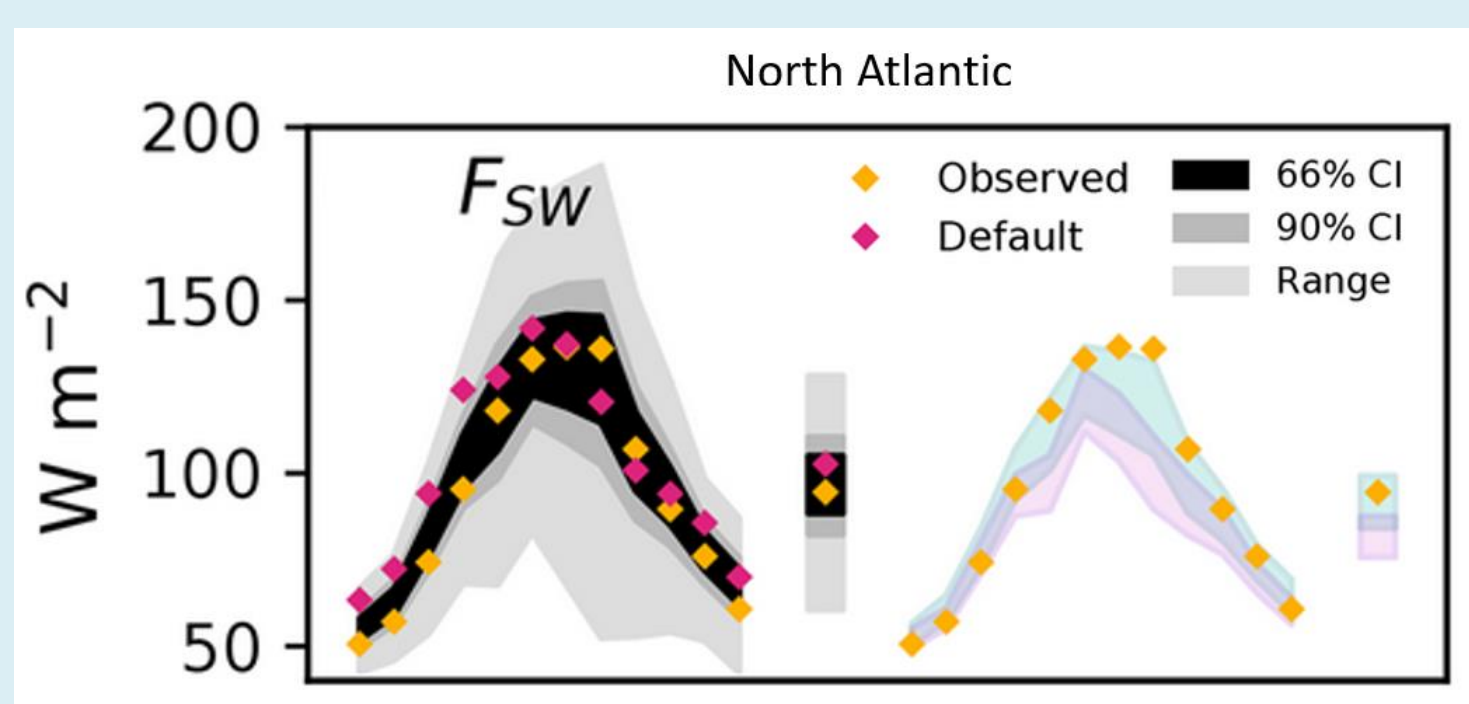


Region	Latitude range	Longitude range
North Atlantic	34.4° to 54.4° N	329.1° to 347.8° E
North Pacific	14.4° to 48.1° N	197.8° to 231.6° E
South Atlantic	30.6° to 10.6° S	347.8° to 2.8° E
South Pacific	30.6° to 15.6° S	254.1° to 284.1° E
Southern Ocean	30.6° to 50.6° S	0° to 360° E

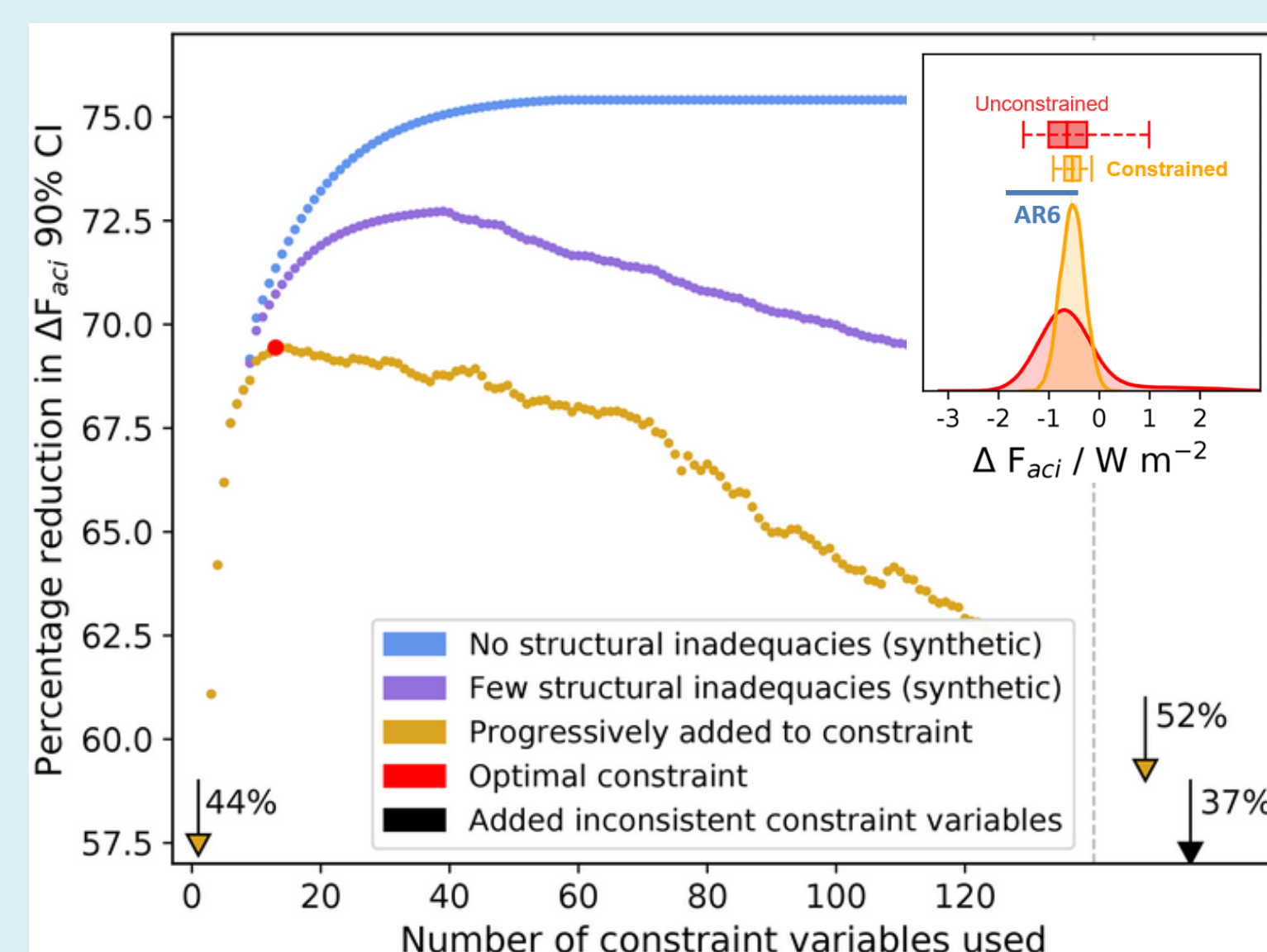
$H_d$ : Hemispheric  $N_d$  contrast  
 T: Sc. to Cu. transects (e.g.,  $dN_d/dLWP$ )  
 $F_{SW}$ : SW flux  
 $F_c$ : cloud fraction  
 $N_d$ : Droplet number  
 $r_e$ : Effective radius  
 $\tau_c$ : Optical depth  
 LWP: Liquid water path

Regayre et al. 2023

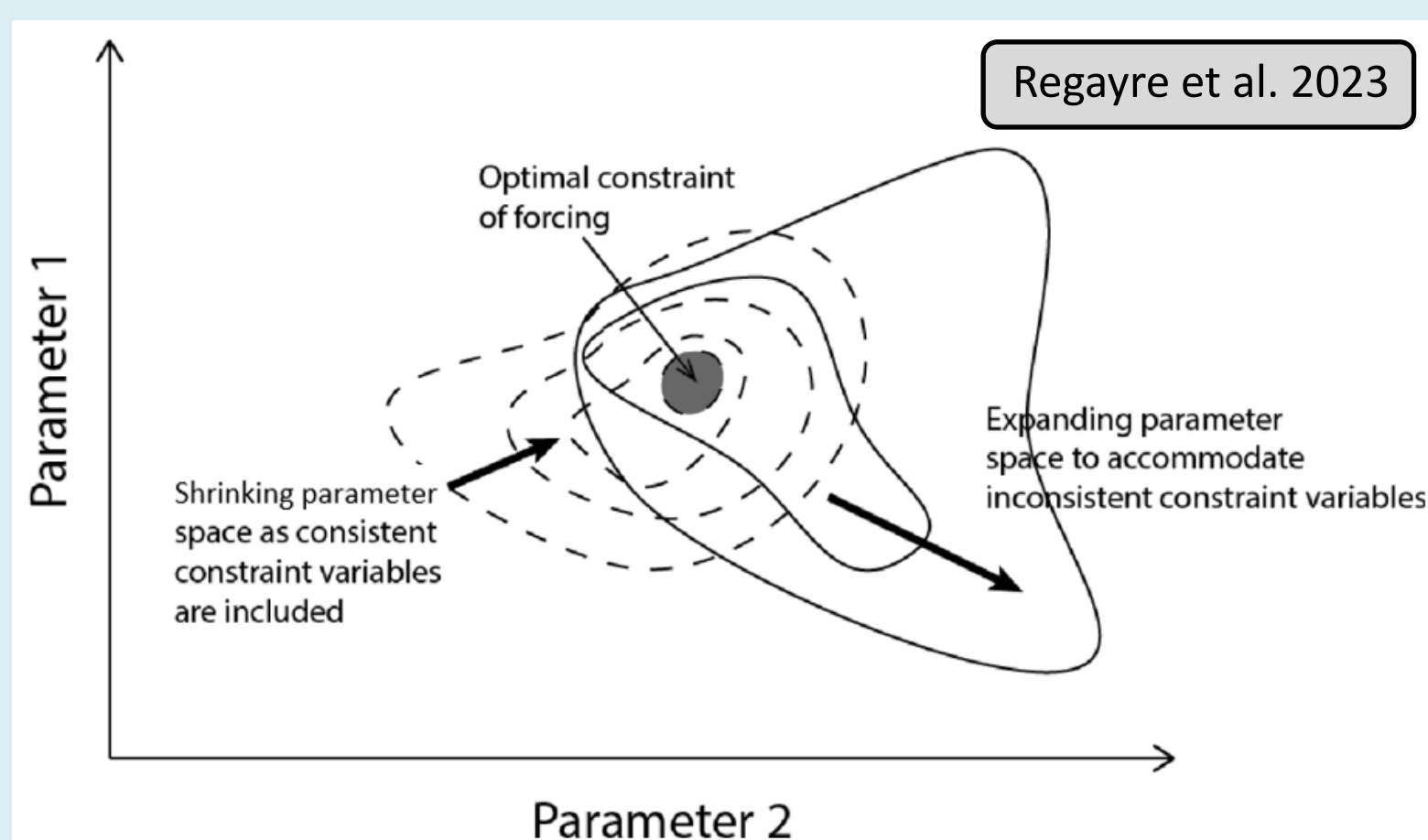
## 3. Exposing the problem of inconsistent constraint effects



The tightest  $\Delta F_{aci}$  constraint ('optimal') needs only 13 observation types, associated with internally consistent model variables



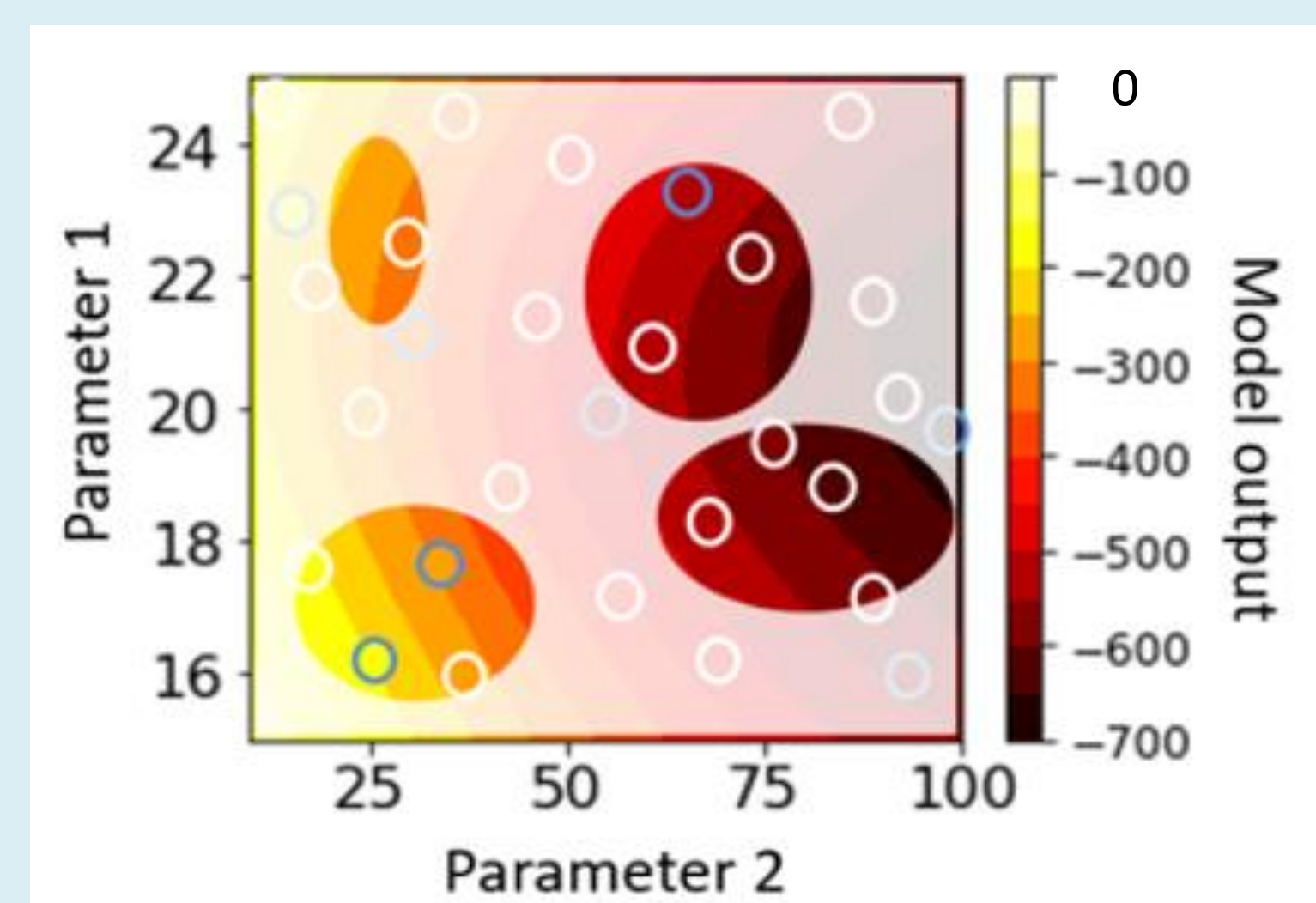
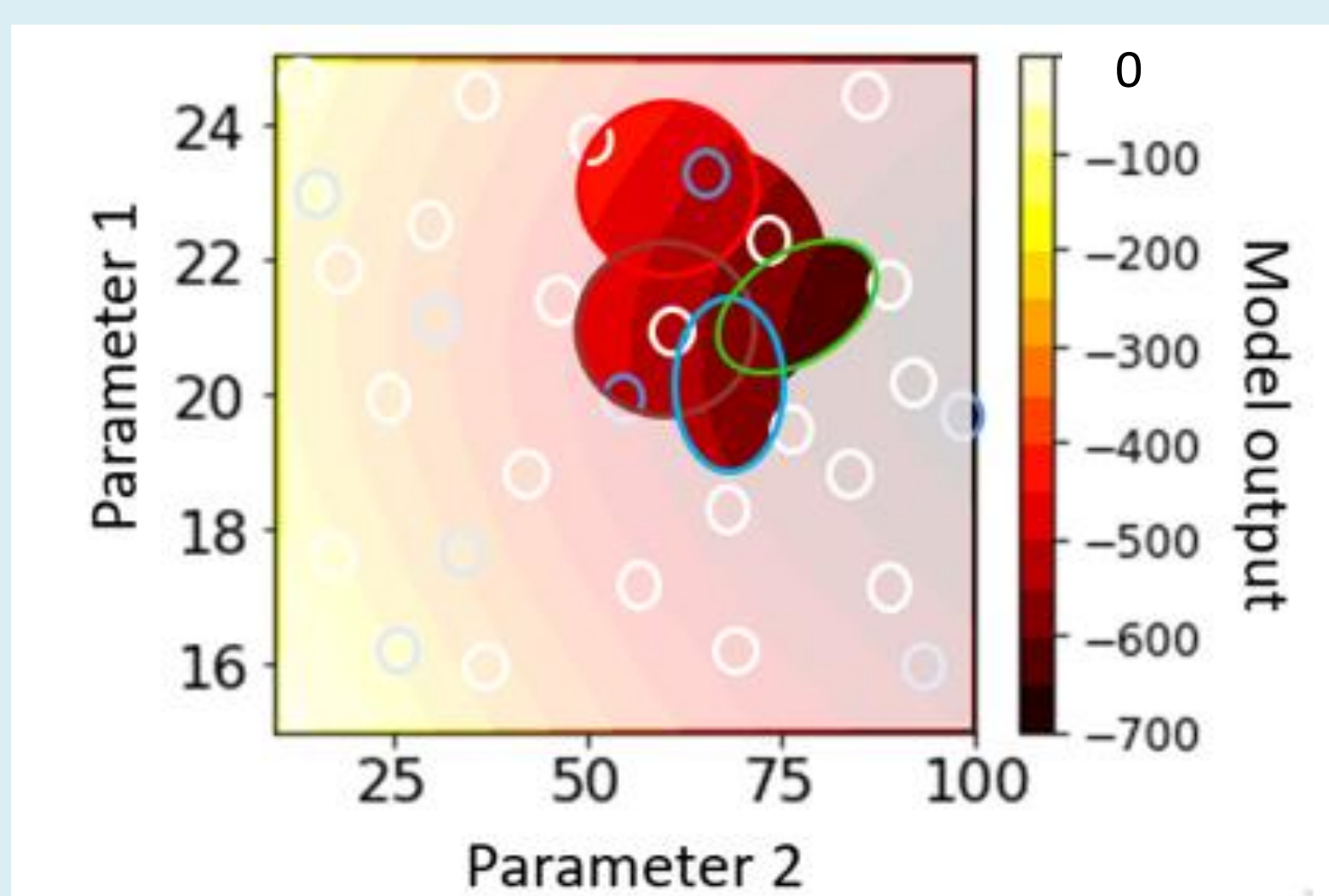
Tight constraint to observed  $N_d$  (green) is consistent with observed  $F_{SW}$  in all months  
 Constraint to LWP (pink) is inconsistent - model  $F_{SW}$  errors increase after LWP constraint



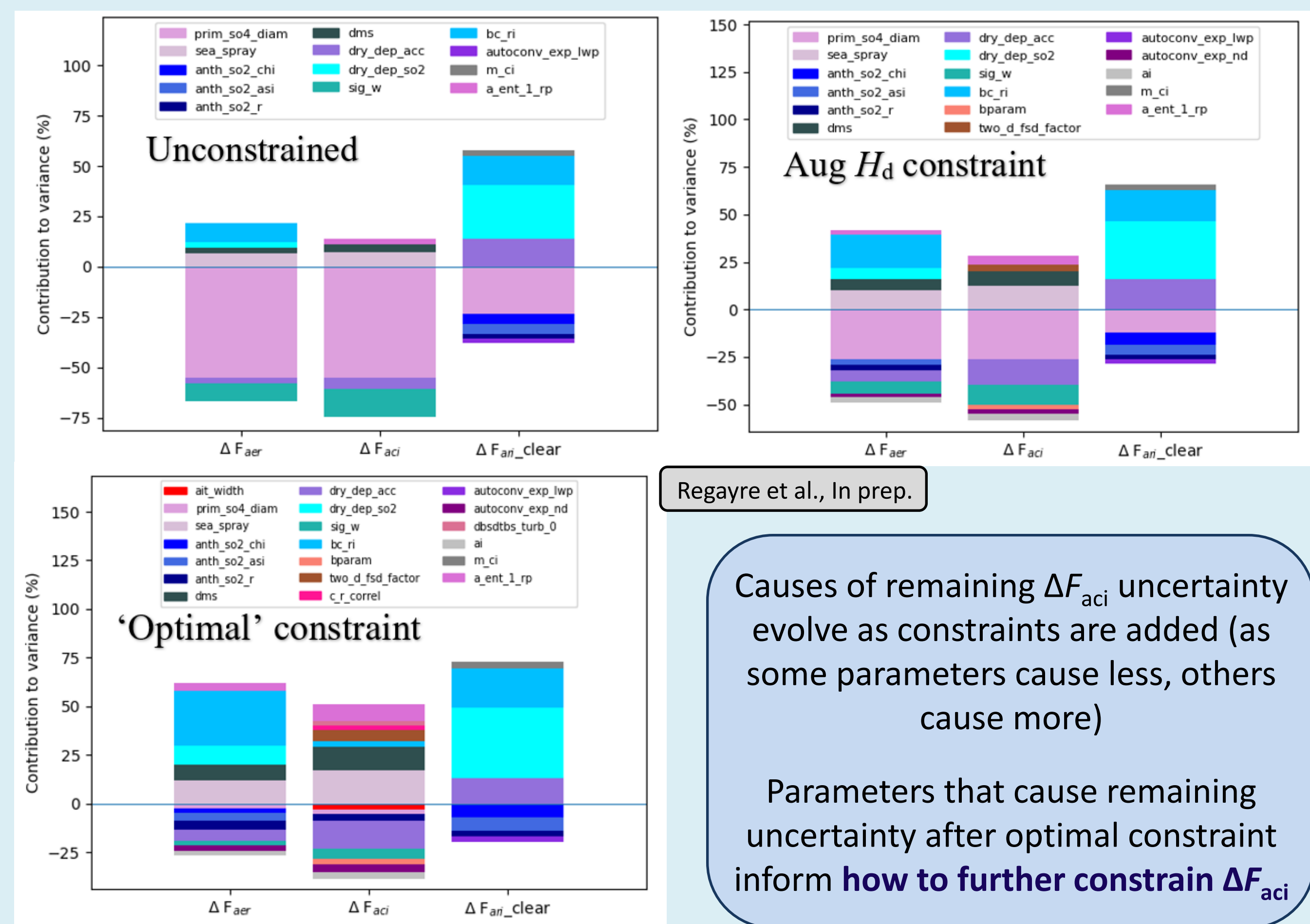
Regayre et al. 2023

Adding further observations demands compromise that reduces the impact of constraint on parameter combinations and weakens  $\Delta F_{aci}$  constraint

More observations could be used for constraint if we had a model free of structural errors



## 4. Effects of constraint on remaining forcing uncertainty



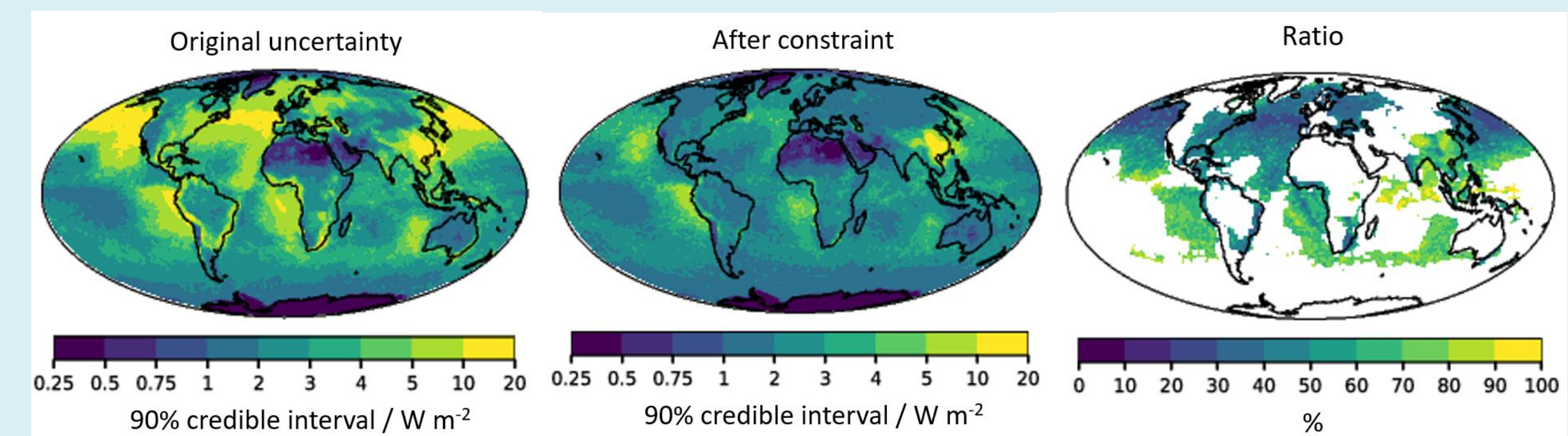
Regayre et al., In prep.

Causes of remaining  $\Delta F_{aci}$  uncertainty evolve as constraints are added (as some parameters cause less, others cause more)

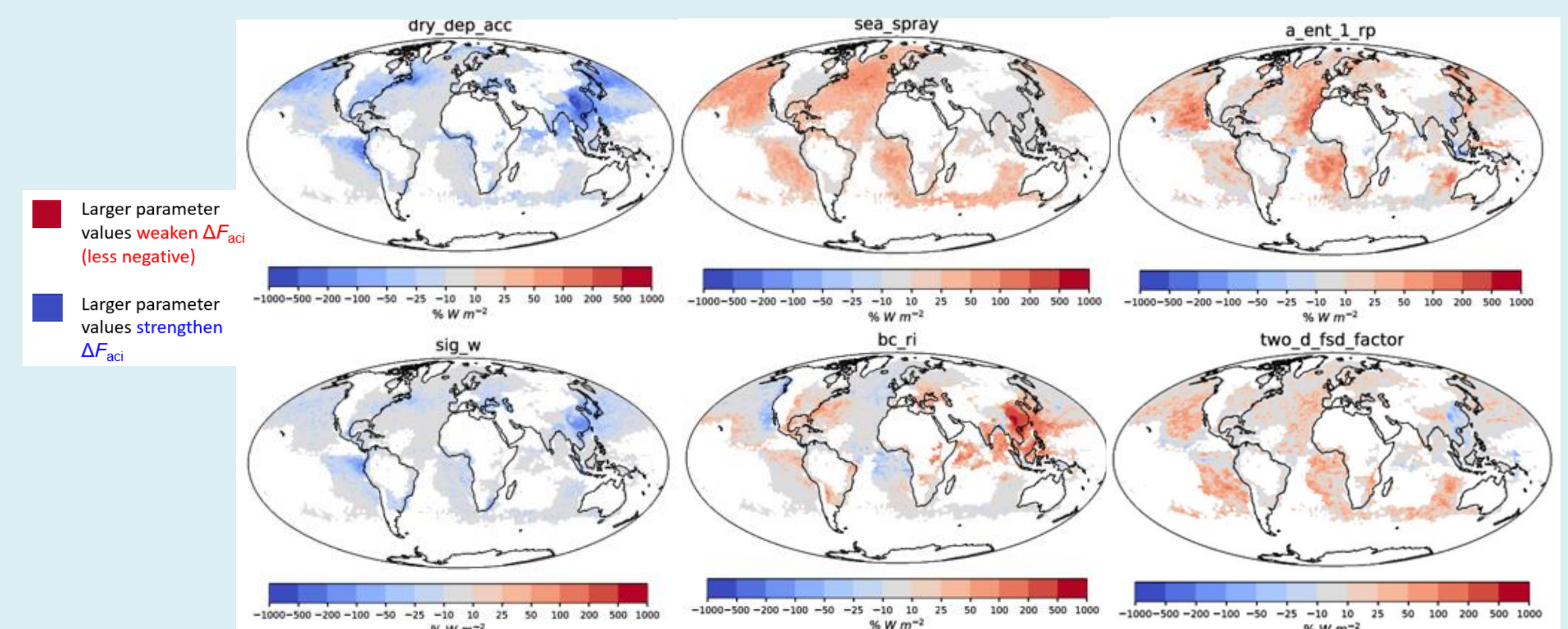
Parameters that cause remaining uncertainty after optimal constraint inform how to further constrain  $\Delta F_{aci}$

## 5. Mapping the causes of remaining uncertainty

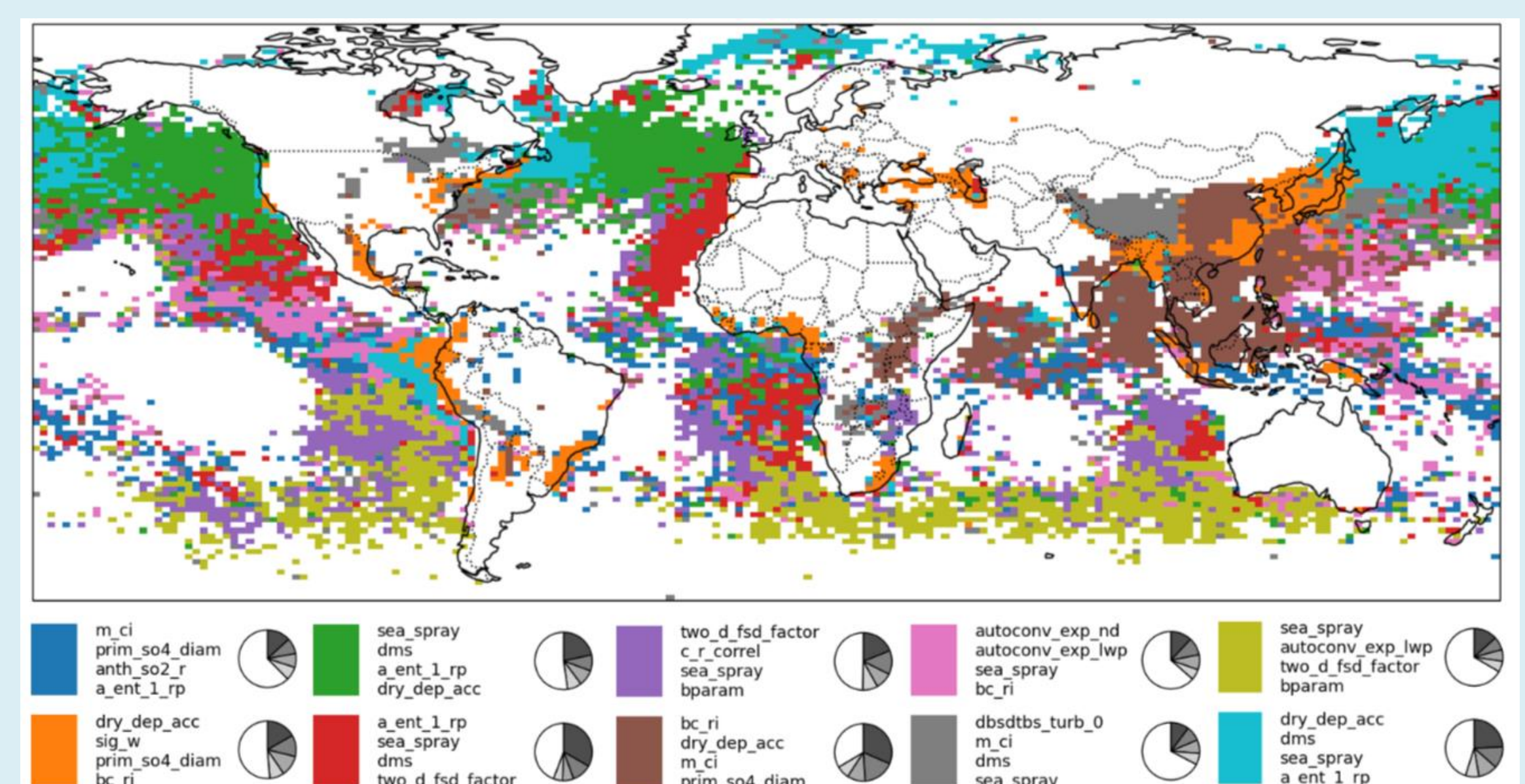
Uncertainty is reduced almost everywhere, with the greatest proportional reduction in N. Hemisphere marine regions. Yet, remaining uncertainty is widespread.



The spatial footprint of causes of remaining  $\Delta F_{aci}$  uncertainty is unique for all 37 model parameters – potential for further constraint partially limited by equifinality



Clusters of model behaviour defined according to combined parametric causes of remaining  $\Delta F_{aci}$  uncertainty after constraint. Useful to group observations for additional  $\Delta F_{aci}$  constraint (as opposed to using regional means)



Regayre et al., In prep.

## 6. Key results

Constraint is stronger when we account for model structural inconsistencies.

We know which parameters cause the remaining  $\Delta F_{aci}$  uncertainty

Additional constraint could be achieved through:

- model developments that target structural inconsistencies
- Use of observations within clusters (targeting parameter combinations)
- Process-based observational constraints (St. to Cu. transitions)